Applied Physics A (2019) 125:24
https://doi.org/10.1007/s00339-018-2322-x

Applied Physics A
Materials Science & Processing

Formation of non-alloyed Ti/Al/Ni/Au low-resistance ohmic contacts on reactively ion-etched n-type GaN by surface treatment for GaN light-emitting diodes applications

Kuldip Singh[1,4] · Ashok Chauhan[1,4] · Manish Mathew[1] · Rajesh Punia[2] · Sher Singh Meena[3] · Nidhi Gupta[3] · Rajender Singh Kundu[4]

Received: 1 August 2018 / Accepted: 8 December 2018 / Published online: 12 December 2018
© Springer-Verlag GmbH Germany, part of Springer Nature 2018

Abstract

Ti/Al/Ni/Au (30/120/20/100 nm) non-alloyed ohmic contacts on reactively ion-etched n-GaN have been obtained by thermal annealing in N_2+O_2 ambient prior to metal contacts deposition. After surface treatment, contacts show the linear current–voltage (*I*–*V*) characteristics with specific contact resistance (SCR) of 2.91×10^{-5} Ω-cm^2 without any post-deposition annealing, whereas, SCR of untreated sample has been found 1.02×10^{-4} Ω-cm^2. The improvement in SCR of Ti/Al/Ni/Au contacts with this process may be attributed to formation of n^+-highly doped layer due to presence of oxygen during thermal annealing. A further increase in SCR of non-treated sample from 1.02×10^{-4} Ω-cm^2 to 3.54×10^{-4} Ω-cm^2, has been observed on further annealing of contacts at 550 °C in N_2+O_2 ambient for 5 min, which is generally an essential condition for formation of low-resistance highly transparent p-contact on p-GaN during fabrication of conventional GaN light-emitting diodes (LEDs). Based on X-ray photoelectron spectroscopy results, we found that there is increase in Ga 3d photoelectron binding energy with this surface treatment, which indicates a shift of Fermi level closure to conduction band, resulting in decrease of Schottky barrier height (SBH). The reduction in SBH is responsible for formation of low-resistance Ohmic contacts on n-GaN. Such non-alloyed n-contacts formed on thermally annealed reactively etched n-GaN surface may open for fabrication of more efficient conventional GaN LEDs. In addition, the forward voltage of GaN LED fabricated by present suggested process lowered by an amount of 0.37 V at 100 mA compared to standard process.

1 Introduction

GaN-based semiconductors have attracted great attention due to their wide applications for optoelectronic devices in ultraviolet, blue, and green wavelength regions. GaN-based light-emitting diodes (LEDs) are playing more and more important role in many applications like back lighting sources, automobile lighting, traffic lights and solid-state lightings [1, 2]. For fabrication of reliable and high-brightness GaN LEDs, low-resistance Ohmic contacts (n and p) are essential. Low-resistance contacts can be easily achieved to p- and n-type GaN layers separately [3–9]. The major problem for these contacts (n and p) arises due to differences in their annealing temperatures and ambient conditions, e.g., for formation of low-resistance (10^{-5}–10^{-6} Ω-cm^2) n-contacts on n-GaN, Ti/Al-based metal stacks are widely used, but this metal stack requires a rapid thermal annealing (RTA) in N_2 ambient in the temperature range of 800–900 °C. Due to the high temperature annealing of these metal contacts, surface morphology of contacts becomes very rough. On the other hand, to form low-resistance contacts on p-type GaN typically requires RTA in the temperature range of 400–600 °C in O_2 or air ambient [10–14].

There are two possibilities to fabricate conventional GaN blue LED chips on sapphire substrates; case-I, n-contact is formed, followed by annealing in the temperature range of 800–900 °C in N_2 ambient to form low-resistance ohmic contact. After annealing, metallic layers are deposited on

✉ Kuldip Singh
kuldip@ceeri.res.in

[1] CSIR-Central Electronics Engineering Research Institute, Pilani 333031, India

[2] Department of Physics, Maharshi Dayanand University, Rohtak 124001, India

[3] Solid State Division, Bhabha Atomic Research Centre, Mumbai 400085, India

[4] Department of Physics, Guru Jambheshwar University of Science and Technology, Hisar 125001, India

p-GaN to form high transparent ohmic contact. However, to form low-resistance highly transparent contacts (> 75% near 460 nm wavelength), it is essential to anneal the p-contact in the temperature range of 400–600 °C in O_2 or air ambient Though, the annealing of p-contacts in O_2 ambient helps to form low-resistance high-transparent ohmic contacts on p-GaN, it degrades the quality of n-contact due to presence of oxygen [15]. On the other hand (case-II), if p-contact is formed earlier than n-contact formation then the annealing of n-contact will degrade the quality of p-contact. It is clear that annealing of n and p-contacts degrades their electrical properties.

In this work, we present a possible solution using different fabrication process sequence for formation of low-resistance Ti/Al/Ni/Au contacts on n-GaN and fabrication of GaN blue LEDs on c-plane sapphire substrate to avoid such degradation of n-contacts due to presence of O_2 during thermal annealing of p-contacts on p-type GaN to form low-resistance high-transparent contacts. In this process, after mesa etching, p-transparent contact is formed prior to n-contact and followed by thermal annealing in $N_2 + O_2$ ambient at 550 °C in RTA to create highly doped n^+-GaN surface and then n-contact is formed. In addition, the electrical and surface properties of Ti/Al/Ni/Au n-contacts on n-GaN were measured and discussed along with electrical properties of fabricated InGaN/GaN MQWs blue LEDs on c-plane sapphire substrate with standard and new process.

2 Experimental details

The epilayer LED structure used in present work was grown by metal organic chemical vapor deposition (MOCVD) system (Thomos Swan 3″ x 2″ CCS) on c-plane sapphire substrate. The LED structure consists of a ~ 25 nm GaN nucleation layer, ~ 2 µm thick undoped GaN, ~ 2 µm thick Si-doped n-GaN, an active region, ~ 30 nm thick Mg-doped AlGaN electron blocking layer (EBL) and 150 nm Mg-doped p-GaN. The active region consists of a five period InGaN/GaN multiquantum wells, embedded between n-GaN and p-GaN layers. The thicknesses of InGaN QW and GaN barrier were about 3 nm and 10 nm, respectively. Trimethylindium (TMIn), gallium (TMGa), trimethylalumium (TMAl) and ammonia (NH_3) were used as the source materials of In, Ga, Al, and N, respectively. Bicylopentadienyl magnesium (CP_2-Mg) and silane (SiH_4) were used as the p-type and n-type dopants. For activation of Mg, grown wafer was annealed at 700 °C for 1 min in N_2 ambient in rapid thermal annealing system. The doping concentration of holes and electrons measured at room temperature by Hall-effect measurement system (Nanometrics HL 5550) were 2×10^{17} cm^{-3} and 4×10^{18} cm^{-3}, respectively. Figure 1 shows the schematic diagram of LED structure used in present study.

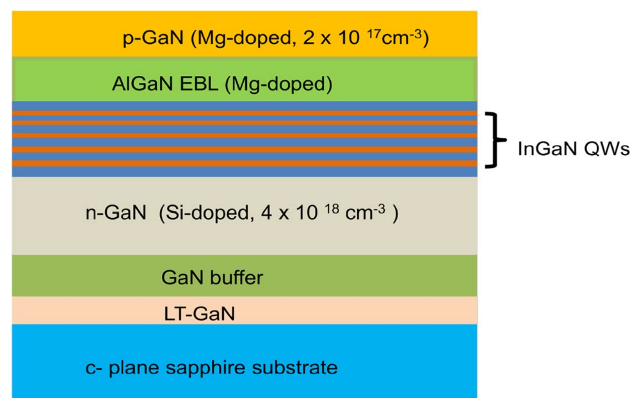

Fig. 1 Schematic diagram of LED structure grown by MOCVD system

Transmission line method (TLM) [16] was used to determine the specific contact resistance of Ti/Al/Ni/Au contacts. To determine the specific contact resistance, first, grown wafer was diced into pieces of ~ 1 cm × 1 cm. To form TLM structure on n-GaN, first epitaxilly grown layers (p-GaN, AlGaN electron blocking layer, InGaN/GaN MQWs and partially n-GaN) were etched in reactive ion etching system (Sentech SI 591). Chlorine chemistry (BCl_3, Cl_2 and Ar) was used for etching of GaN layers. After reactive ion etching, one sample was thermally treated at 550 °C for 5 min in $N_2 + O_2$ ambient in rapid thermal annealing system (Annealsys As-One 100) while, other was kept untreated. After reactive ion etching, TLM structures with pads of size 200 µm × 200 µm with contact spacing 5, 10, 15, 20, 25 and 30 µm were defined by UV lithography on these two samples. Before loading the samples in e-beam chamber, samples were pre-etched in HCl and de-ionized water solution in ratio of 1:1 for 1 min to remove the native oxide on n-GaN surface. After pre-etching, both samples were loaded in chamber of electron beam evaporation system (VST TFDS 462B). Ti/Al/Ni/Au (30/120/20/100 nm) multilayer metals were evaporated by e-beam system at the base pressure of 1.3×10^{-6} Torr. After deposition of metal layers, lift-off process was carried out for realization of TLM contact pads. Figure 2 shows the detailed process sequences for formation of n-contacts.

Current–voltage (*I*–*V*) data were measured using probe station (Ecopia EPS-1000). The surface morphology of n-GaN surface and Ti/Al/Ni/Au contacts were evaluated by means of atomic force microscopy (CSI-Nano Observer) and scanning electron microscopy (JEOL JCM 5700). VG make CLAM 2 system was used for X-ray photoelectron spectroscopy (XPS) to explain the effect of thermal treatment on specific contact resistance.

To study the impact of Ti/Al/Ni/Au n-contacts formed on reactively ion-etched n-GaN with different processes

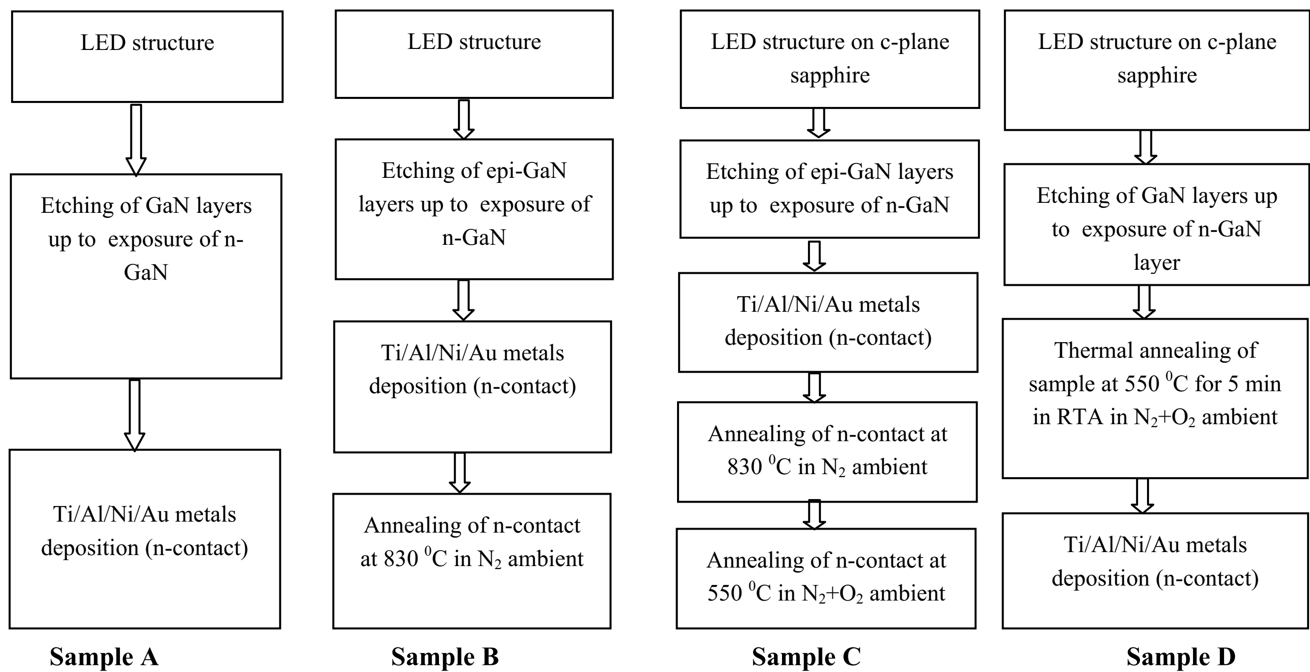

Fig. 2 Illustration of process sequences for formation of contacts with standard and new processes

on electrical properties of LEDs, InGaN/GaN MQWs blue LEDs on c-plane sapphire substrate with two processes were also fabricated. For fabrication of LEDs, mesa etch was performed in both samples by reactive ion etching and followed by HCl:H_2O clean. For mesa etching, photoresist (Shipley-1818) was used as masking layer. In standard GaN LED fabrication process, n-contact metals (Ti/Al/Ni/Au) were evaporated by e-beam, followed by annealing at 830 °C for 30 s in N_2 ambient. The transparent p-contact (Ni/ITO, 5/50 nm) was then evaporated and followed by annealing at 550 °C for 5 min in N_2+O_2 ambient. After formation of transparent p-contact, p-pad (Ti/Au, 30/200 nm) was formed for electrical connections. In present process, after mesa etch, the p-metals (Ni/ITO, 5/50 nm) were evaporated first, followed by annealing at 550 °C for 5 min in N_2+O_2 ambient. This annealing step also serves as the surface treatment on n-GaN surface before deposition of n-contact metals. The n-contact metals (Ti/Al/Ni/Au) were then evaporated. No post-deposition annealing at higher temperature in N_2 ambient was performed. Figure 3 shows the detailed fabrication process flow of GaN LEDs on sapphire substrate with standard and new process.

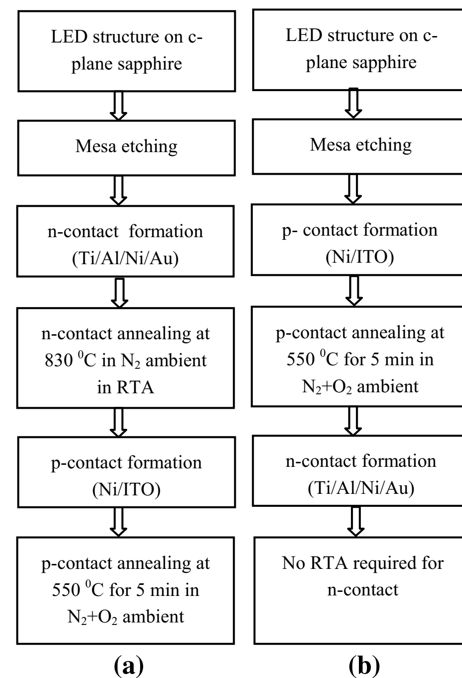

Fig. 3 GaN LED fabrication; **a** standard **b** new process

3 Results and discussion

The electrical characterization of contacts was performed by means of current–voltage (*I*–*V*) measurements using TLM structures. Figure 4 shows the room temperature *I*–*V* characteristics of contacts, measured between two adjacent TLM pads with a gap spacing of 10 µm. It is clear that as-deposited n-metals on reactively ion-etched n-GaN (sample A, red circles), exhibits a nonlinear *I*–*V* behaviour, i.e., rectifying behavior. This rectifying behavior

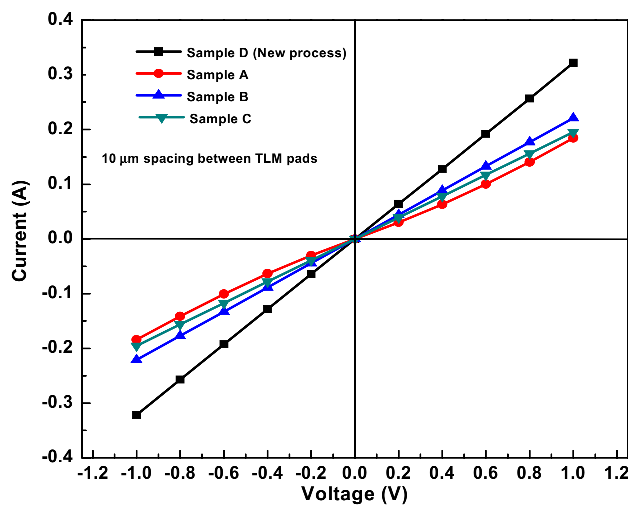

Fig. 4 Room temperature *I–V* characteristics of Ti/Al/Ni/Au contacts using TLM pads with gap spacing of 10 µm with standard and new processes

may be attributed to a large Schottky barrier between Ti and GaN [17]. After rapid thermal annealing (RTA) of contacts at 830 °C for 30 s in N_2 ambient, the *I–V* behaviour of contacts becomes linear, i.e., Ohmic (sample B, blue triangles). This linear behavior may be attributed to formation of a highly doped TiN [18–20], Al_3Ti [21] and other microstructural changes, e.g., formation of Al–Ni grains, Al–Au phases such as Al_2Au and AlTi(Au) compound [20] during RTA at higher temperatures. During annealing of contacts at higher temperature, out-diffusion of N atoms from GaN leads the formation of N vacancies. These N vacancies produced a very thin highly n-doped interfacial layer. The formation of such highly doped TiN interface layer and other microstructural changes not only reduces the Schottky barrier height (SBH) but increases the contact area of contacts and thus, leads to form the linear *I–V* behavior. Further, the *I–V* curve of contacts degraded, when they were further annealed at 550 °C in N_2+O_2 ambient, which is an essential condition for standard GaN LEDs fabrication (sample C, inverted triangle). The possible cause of degradation of *I–V* behavior of contacts may be attributed to oxidation of Al and to form a very thin layer of Al_2O_3 during annealing, because Al can be easily oxidized in the presence of oxygen at higher temperature. On the other hand, the *I–V* curve of contacts with new process shows better and linear characteristics, i.e., Ohmic even without any high-temperature annealing after deposition of contacts on reactively ion-etched n-GaN surface (sample D, black squares). The ohmic behaviour of contacts may be due to formation of highly n^+-doped surface on n-GaN as a result of thermal annealing at 550 °C in N_2+O_2 ambient after reactive ion etching, because oxygen is well known donor for GaN material [22]. This highly n^+-doped surface reduces the SBH between metal (Ti) and n-GaN, resulting in the increase in tunneling of electrons through the barrier. The increase in tunneling of electrons through barrier is a cause of formation of ohmic contacts.

The specific contact resistances (SCR) of contacts were extracted from TLM data. Table 1 shows the specific contact resistances of Ti/Al/Ni/Au contacts made on reactively ion-etched n-GaN material with different conditions. The SCR of sample B (without thermal treatment) was found 1.02×10^{-4} Ω-cm^2. However, when these contacts were further annealed in N_2+O_2 ambient at 550 °C for 5 min, as described in Fig. 3a, it was found that SCR was increased from 1.02×10^{-4} to 3.54×10^{-4} Ω-cm^2, i.e., nearly 3.5 times increase in SCR. The further annealing step is an essential condition for formation of low-resistance highly transparent ohmic contacts to p-GaN during standard GaN LED fabrication process. The increase in SCR of further annealed contacts in N_2+O_2 ambient may be attributed again to formation of a very thin layer of Al_2O_3 during annealing [23, 24]. However, SCR of thermally treated sample D was obtained as 2.91×10^{-5} Ω-cm^2, i.e., nearly 3.5 times lower compared to standard process for n-contact formation (sample B). This is the lowest value reported for non-alloyed contacts on n-GaN [15, 25, 26]. This reduction in SCR of thermally treated contacts may be again attributed to reduction of SBH between Ti and n-GaN because, during thermal treatment of n-GaN in N_2+O_2 ambient in RTA, because oxygen creates additional donors at the top of n-GaN surface.

Table 1 Specific contact resistance of Ti/Al/Ni/Au contacts on reactively ion-etched n-GaN under different conditions

Process	Specific contact resistance (Ω-cm^2)
RIE of LED structure up to exposure of n-GaN/Ti/Al/Ni/Au contact formation/contact annealing at 830 °C N_2 ambient (standard process for n-ohmic contact formation)	1.02×10^{-4}
RIE of LED structure up to exposure of n-GaN/Ti/Al/Ni/Au contact formation/ annealing of contact at 830 °C N_2 ambient/ annealing at 550 °C N_2+O_2 ambient (standard GaN LED fabrication process)	3.54×10^{-4}
RIE of LED structure up to exposure of n-GaN/thermal annealing at 550 °C in N_2+O_2 ambient /Ti/Al/Ni/Au contact formation/no annealing of contacts (New LED fabrication process)	2.91×10^{-5}

To analyze the surface morphology of n-GaN surface for non-treated and thermally treated samples, atomic force microscopy was performed. Figure 5a, b shows the AFM images of reactive ion-etched n-GaN surface before and after thermal annealing of n-GaN samples. The root mean square (RMS) roughness for non-treated n-GaN surface was 23.646 nm. On the other hand, RMS roughness of thermally treated n-GaN surface was 41.179 nm. The increase in surface roughness after thermal treatment of n-GaN surface may be related to the formation of new surface structure, i.e., surface might undergo reconstruction and turn to the ordered structure. The energy needed for reconstruction of surface is provided by thermal annealing. The surface morphology of Ti/Al/Ni/Au contacts was also characterized by scanning electron microscopy (SEM). Figure 6 shows the change in surface morphology of contacts on n-GaN under different process measured by SEM. Figure 6a shows the SEM image of annealed Ti/Al/Ni/Au contacts at 830 °C for 30 s in N_2 ambient, Fig. 6b shows SEM image of contacts annealed in two steps, i.e., first annealed at 830 °C for 30 s in N_2 ambient and followed by 550 °C for 5 min in N_2+O_2 ambient, while Fig. 6c shows the SEM image of contacts, which were formed on thermally annealed (550 °C for 5 min in N_2+O_2 ambient) reactively ion-etched n-GaN surface without post-deposition annealing of contacts. However, surface of annealed contacts at 830 °C was very rough. The pits can be seen on the n-GaN surface (Fig. 6a). One of the major causes of such roughed surface of contacts is due to balling up of melted Al and surface burst due to low melting point of Al (~660 °C) metal [19, 24]. The other probable causes of roughed surface of contacts after annealing may be attributed to intermixing of metals and formation of different phases like Au–Al–Ti, Al_2Au, AlNi etc, during annealing [20]. The roughness of contacts further increased when, contacts were further annealed at 550 °C for 5 min in N_2+O_2 ambient (Fig. 6b). The increase in roughness of contacts may be attributed to reaction of O_2 with different phases formed during annealing. From SEM image (Fig. 6c), it is clear that balling up problem can be eliminated using present suggested process for formation of Ti/Al/Ni/Au contacts on

Fig. 5 AFM images of reactive ion-etched n-GaN surface; **a** non-treated, **b** treated samples

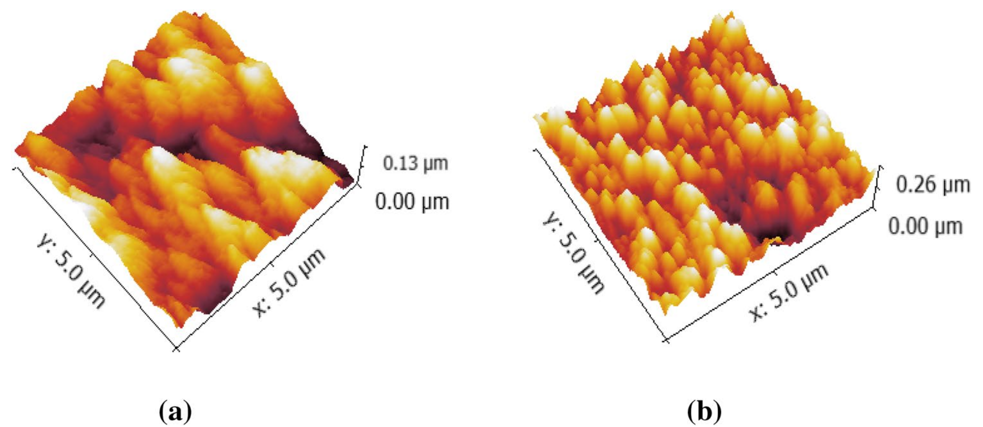

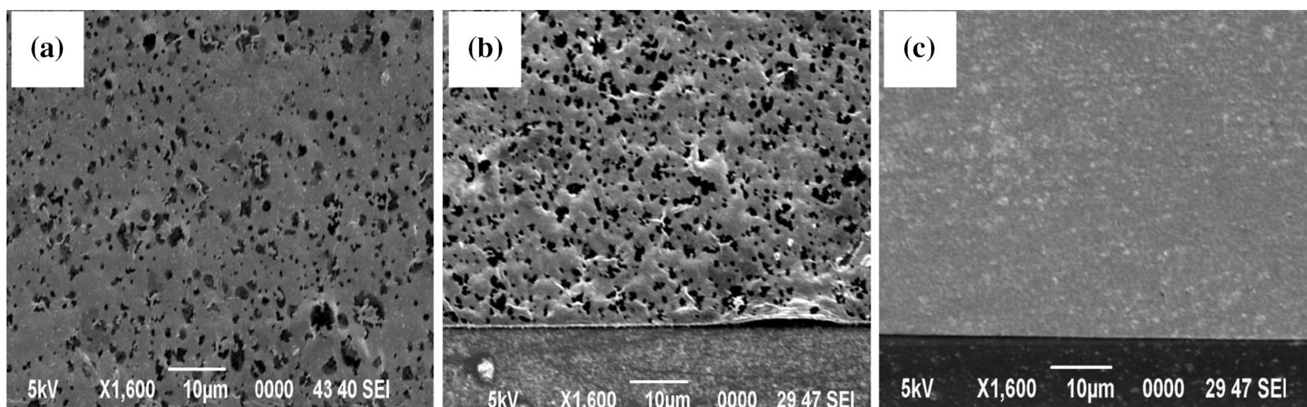

Fig. 6 SEM images of Ti/Al/Ni/Au contacts; **a** formed on reactively ion-etched n-GaN and then annealed at 830 °C in N_2 ambient, **b** two-step annealed, i.e., first at 830 °C in N_2 ambient and then at 550 °C for 5 min in N_2+O_2 ambient (as in case of standard LED fabrication process), **c** formed on thermally treated n-GaN surface (new process)

reactively ion-etched n-GaN surface. The smooth surface obtained with this new process may be attributed to no further annealing requirement after deposition of Ti/Al/Ni/Au contacts.

To investigate the effect of $N_2 + O_2$ thermal annealing on reactively ion-etched n-GaN surface, an A1 Kα X-ray source of energy 1486.6 eV was used to characterize the surface analysis. The samples were scanned from energy range 0–1000 eV at vacuum of 1×10^{-8} Torr at Fig. 7 shows the XPS survey spectra for treated and untreated n-GaN samples. The C 1 s peaks are at 284.44 eV and 284.49 for untreated and treated samples. Since change in binding energy after thermal treatment is almost negligible, therefore, it may be assumed that after treatment, the hydrocarbon contaminants are almost same on n-GaN surface. Since the Ga 3d core-level peak is closely associated with the surface Fermi level (E_F) position, hence, XPS spectra of the Ga 3d photoelectrons for treated and untreated n-GaN samples are important. Figure 8 shows the high-resolution XPS spectra of Ga 3d photoelectrons for thermally treated in $N_2 + O_2$ ambient and untreated n-GaN samples. The black line and red line (dotted) show the experimental and fitted data. The peak of Ga 3d (GaN) photoelectron for non-treated sample is positioned at 19.384 eV. On the other hand, the peak of Ga 3d (GaN) photoelectron for treated sample is positioned at 19.613 eV. From XPS data, it is clear that peak for Ga 3d shifts by 0.229 eV towards higher binding energy for thermally treated n-GaN sample. For detailed surface analysis of treated sample, Ga 3d peak was deconvoluted into three peaks, Ga–N, Ga–O and Ga–Ga metal. Figure 9 shows the deconvoluted XPS spectra of Ga 3d for thermally treated n-GaN sample. It is clear that Ga–Ga (18.68 eV) and Ga–O (20.69 eV) peaks were clearly observed. The high-resolution XPS spectra of O 1 s photoelectrons for thermally treated and untreated samples are shown in Fig. 10. From XPS data of O 1 s photoelectrons, it is clear that peak intensity corresponding to O 1 s photoelectrons increases for thermally treated n-GaN sample.

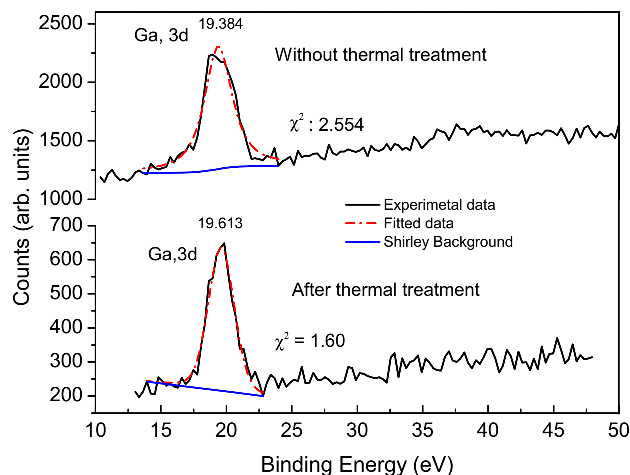

Fig. 8 XPS spectra of Ga 3d at the surface of n-GaN for non-treated and treated samples

The shift of the Ga 3d core-level peak to higher binding energy indicates the shifting of Fermi level towards the conduction band edge, resulting in a creation of highly n^+-doped layer on the reactively ion-etched n-GaN surface. This phenomenon is responsible for decrease of SBH between Ti and GaN. Thus, from XPS data, it is clear that thermal treatment of reactive ion-etched n-GaN surface in $N_2 + O_2$ ambient at 550 °C leads to form non-alloyed Ti/Al/Ni/Au metal-based low-resistance Ohmic contacts on n-GaN.

Figure 11 shows room temperature *I–V* characteristics of fabricated GaN blue LEDs with standard and new process. It is clear that LEDs fabricated with new process has better *I–V* characteristics. This better *I–V* of LED device with new process may be attributed to lower series resistance of

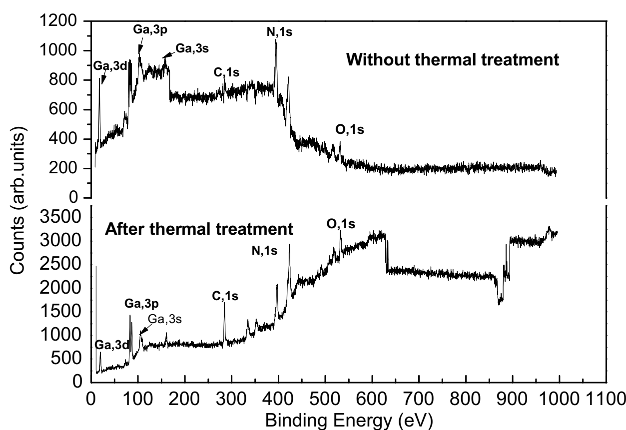

Fig. 7 XPS survey spectra of non-treated and treated n-GaN samples

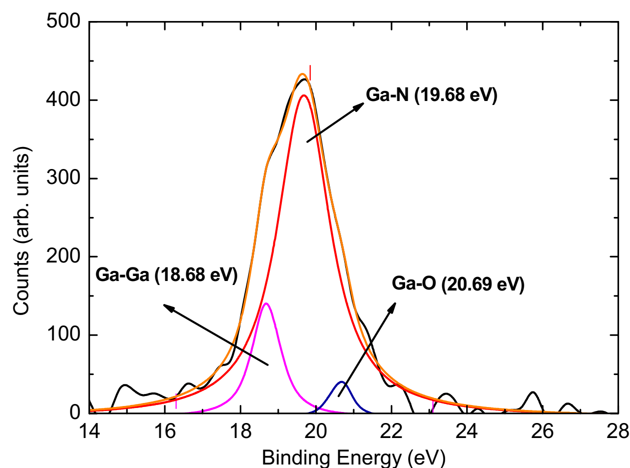

Fig. 9 Deconvoluted XPS spectra Ga 3d of treated sample

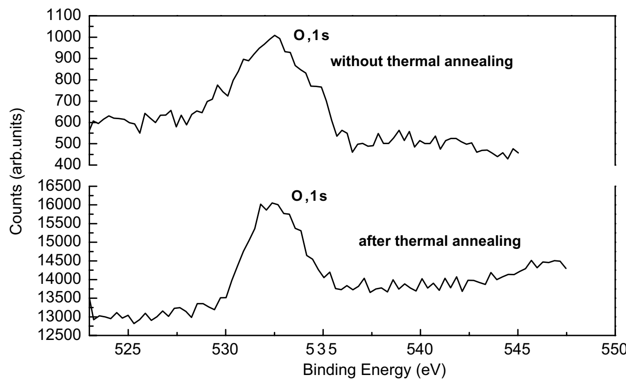

Fig. 10 XPS spectra of Ga 3d at the surface of n-GaN for non-treated and treated samples

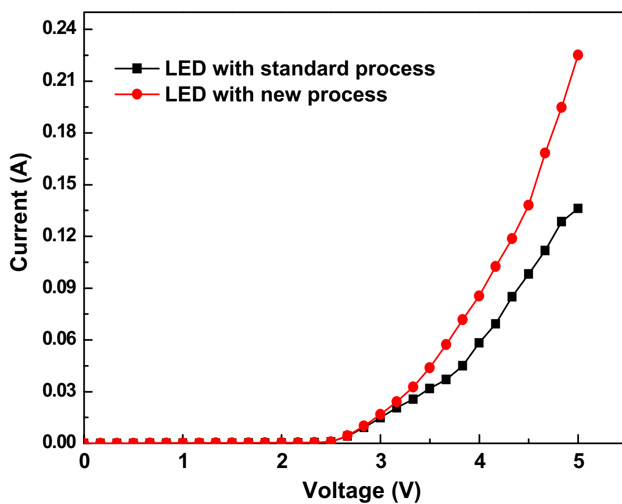

Fig. 11 *I–V* characteristics of GaN blue LEDs with standard and new process

device, because SCR of n-contact with new process was 2.91×10^{-5} Ω-cm^2, which was ~ 12 times lower (3.54×10^{-4} Ω-cm^2) compared to standard process. It is well known that the forward voltage of GaN LED devices depends on device series resistance and in-device series resistance, the SCR of n- and p-contacts has major contribution. In new process, the SCR of n-contact (one of the major components of device resistance) was achieved much lower compared to standard process. Due to lower SCR of n-contacts with new process, forward voltage of LED device at injection current of 100 mA, was about 0.37 V lower compared to LED with standard process. Thus, with new process, not only the better surface morphology of contacts has been achieved but post-deposition annealing is also not required as in case of standard process. These results indicate that significant improvements in the performance of the n-type contacts were achieved with new process. RTA annealing in N_2+O_2 ambient at 550 °C as generally used for p-metal contact annealing for formation of low-resistance and high-transparent ohmic contacts on p-GaN, also assists in the formation of non-alloyed Ti/Al/Ni/Au ohmic contacts on n-GaN without any post-deposition annealing.

4 Conclusions

In presented work, non-alloyed Ti/Al/Ni/Au ohmic contacts on reactively ion-etched n-GaN surface have been successfully deposited with a different approach. The new surface treatment consisting of RTA at 550 °C in N_2+O_2 ambient for 5 min on reactively ion-etched n-GaN creates a highly doped n-GaN surface at metal–semiconductor interface, which is responsible for formation of non-alloyed ohmic contacts on n-GaN. This process of formation of ohmic contacts on n-GaN is found better than n-contact annealed in RTA at higher temperature in N_2 ambient. The SCR of Ti/Al/Ni/Au n-contacts with new process is ~ 3.5 times lower (2.91×10^{-5} Ω-cm^2) compared to n-contact formed on reactively ion-etched n-GaN (1.02×10^{-4} Ω-cm^2) and ~ 12 times lower for process adopted for standard LED process. Moreover, the surface morphology of n-GaN treated with new process is much better as compared to the standard GaN LED fabrication process due to absence of post-deposition annealing of Ti/Al/Ni/Au contacts at 830 °C in N_2 ambient. XPS analysis shows that the Fermi level at n-GaN surface shifts towards the conduction band edge for thermally treated n-GaN sample in N_2+O_2 ambient, which results in a reduction of SBH and SCR. With new process, the forward voltage of fabricated GaN blue LED at 100 mA is lower by ~ 0.37 V compared to the standard process. It means that series resistance of LED device is lowered by significant amount with new process. These results strongly indicate that new process may be suitable for the fabrication high-performance GaN LEDs.

Acknowledgements This work was supported by council of scientific and industrial research (CSIR), New Delhi, India under network programme (PSC-0102).

References

1. M. Koike, N. Shibata, H. Kato, Y. Takahashi, IEEE J. Sel. Top. Quantum Electron. **8**, 271–277 (2002)
2. S.P. DenBaars, D. Feezell, K. Kelchner, S. Pimputkar, C.-C. Pan, C.C. Yen, S. Tanaka, Y. Zhao, N. Pfaff, R. Farrell, M. Iza, S. Kelkar, U. Mehra, J.S. Speck, S. Nakamura, Acta Mater. **61**, 945–951 (2013)
3. M.E. Lin, Z. Ma, F.Y. Huang, Z.F. Fan, L.H. Allen, H. Morkoc, Appl. Phys. Lett. **64**, 1003–1005 (1994)
4. J.K. Ho, C.S. Jong, C.C. Chiu, C.N. Huang, K.K. Shih, L.C. Chen, F.R. Chen, J.J. Kai, J. Appl. Phys. **86**, 4491–4497 (1999)

5. D.-F. Wang, F. Shiwei, C. Lu, A. Motayed, M. Jah, S.N. Mohammad, J. Appl. Phys. **89**, 6214–6217 (2001)
6. D.H. Youn, M.S. Hao, H. Sato, T. Sugahara, Y. Naoi, S. Sakai, Jpn. J. Appl. Phys. **37**, 1768–1771 (1998)
7. J.O. Song, J.-S. Ha, T.-Y. Seong, IEEE Trans. Electron Devices **57**, 42–59 (2010)
8. G. Greco, F. Iucolano, F. Roccaforte, Appl. Surf. Sci. **383**, 324–345 (2016)
9. F. Lin, B. Shen, S. Huang, F.J. Xu, H.Y. Yang, W.H. Chen, N. Ma, Z.X. Qin, G.Y. Zhang. 9th International Conference on Solid-State and Integrated-Circuit Technology (2008), pp 726–729
10. J.S. Kwak, J. Cho, S. Chae, O.H. Nam, C. Sone, Y. Park, Jpn. J. Appl. Phys. **40**, 6221–6225 (2001)
11. S.Y. Kim, H.W. Jang, J.-L. Lee, Appl. Phys. Lett. **82**, 61–63 (2003)
12. S.Y. Kim, H.W. Jang, J.-L. Lee, Phys. Stat. Sol. (c) **0**, 214–218 (2002)
13. R.-H. Horng, D.-S. Wuu, Y.-C. Lien, W.-H. Lan, Appl. Phys. Lett. **79**, 2925–2927 (2001)
14. J.O. Song, K.-K. Kim, H. Kim, H.-G. Hong, H. Na, T.-Y. Seong, Electrochem. Solid State Lett. **10**, H270–H272 (2007)
15. W. Hou, T. Detchprohm, C. Wetzel, Int. J. High Speed Electron. Syst. **20**, 521–525 (2011)
16. G.K. Reeves, H.B. Harrision, IEEE Electron Device Lett. **3**, 111–113 (1982)
17. W. Hou, T. Detchprohm, C. Wetzel, Appl. Phys. Lett. **101**, 242105-1–242105-4 (2012)
18. S. Ruvimov, Z. Liliental-Weber, J. Washburn, K.J. Duxstad, E.E. Haller, Z.F. Fan, S.N. Mohammad, W. Kim, A.E. Botcharev, H. Morkoc, Appl. Phys. Lett. **69**, 1556–1558 (1996)
19. L. Pang, K. Kim, Mater. Sci. Semicond. Process. **29**, 90–94 (2015)
20. F. Iuconao, F. Roccaforte, A. Alberti, C. Bongiorno, S. Di Franco, V. Raineri, J. Appl. Phys. **100**, 123706-1–123706-8 (2006)
21. A.V. Davydov, A. Motayed, W.J. Boettinger, R.S. Gates, Q.Z. Xue, H.C. Lee, Y.K. Yoo, Phys. Stat. Sol. (c) **2**, 2551–2554 (2005)
22. C. Wetzel, T. Suski, A.W. Ager, E.R. Weber, E.E. Haller, S. Fischer, B.K. Meyer, R.J. Molnar, P. Perlin, N. Koike, H. Shibata, Kato, Y. Takahashi, Phys. Rev. Lett. **78**, 3923–3926 (1997)
23. A. Motayed, M.C. Wood, O.S. Diouf, R.D. Vispute, S.N. Mohammad, J. Appl. Phys. **93**, 1087–1094 (2003)
24. Z. Fan, S.N. Mohammad, W. Kim, Ö Aktas, A.E. Botchkarev, H. Morkoc, Appl. Phys. Lett. **68**, 1672–1674 (1996)
25. H.K. Cho, S.-K. Kim, J.S. Lee, J. Phys. D Appl. Phys. **41**, 175107 (2008)
26. M.-L. Lee, J.-K. Sheu, C.C. Hu, Appl. Phys. Lett. **91**, 182106-1–182106-3 (2007)